SLAC – PUB – 3818
October 1985
(E)

RECENT RESULTS ON D MESON DECAYS FROM THE MARK III*

David H. Coward
Stanford Linear Accelerator Center
Stanford University, Stanford, California 94305

Representing the MARK III Collaboration

1. INTRODUCTION

The MARK III Collaboration recently completed the analysis of a number of decay modes of charged and neutral D mesons produced in electron-positron collisions near the peak of the $\psi(3770)$ resonance at SLAC's SPEAR storage ring. The mesons were produced nearly at rest in pairs, either D^+D^- or $D^0\bar{D}^0$, at a center-of-mass energy below the threshold for DD^* production. The unique kinematics of the production allow us to isolate the charmed meson signal clearly and unambiguously. The data were collected with the MARK III Spectrometer, a large solid angle magnetic detector which has been described in detail elsewhere.[1] Our data sample corresponds to an integrated luminosity of approximately 9.3 inverse picobarns.

New results will be presented on the absolute branching ratios of D mesons into hadronic final states, branching ratios for three body decays via pseudoscalar-vector intermediate states, and branching ratios for Cabibbo allowed and Cabibbo suppressed decays. Inclusive and exclusive branching ratios for the semi-leptonic decays of D mesons will be presented, as well as the first measurement of the vector form factor in the decay $D^0 \to K^-e^+\nu$, evidence for interference in D^+ decays, and new information on the contributions of W exchange diagrams to D^0 decays.

2. ABSOLUTE BRANCHING RATIOS TO HADRONIC FINAL STATES

Since charmed D mesons are produced in pairs in our data sample, we can make a unique identification of the charm of a single D meson through the reconstruction of the hadronic decay of the D or $\bar{D}$. These reconstructed events form our single-tag sample, containing 3435 D^0 and 1729 D^+ mesons. We then study the decay of the recoil $\bar{D}$ or D meson, and determine their absolute

* Work supported in part by the National Science Foundation and by the Department of Energy, contracts DE-AC03-76SF00515, DE-AC02-76ER01195, DE-AC03-81ER40050, and DE-AM03-76SF00034.

Invited talk presented at the Annual Meeting of the Division of Particles and Fields of the APS, Eugene, Oregon, August 12-15, 1985

branching ratios into hadrons, electrons or muons. These events with both D's reconstructed give us our double-tag sample. Here and throughout this paper, we adopt the convention that reference to a particle state also implies reference to its charge conjugate. Because of the good mass resolution of the MARK III detector, we have a very clean sample of tagged charm events. In Fig. 1 we show mass plots for 105 D^+ and 367 D^0 double-tag combinations into the listed hadronic final states.

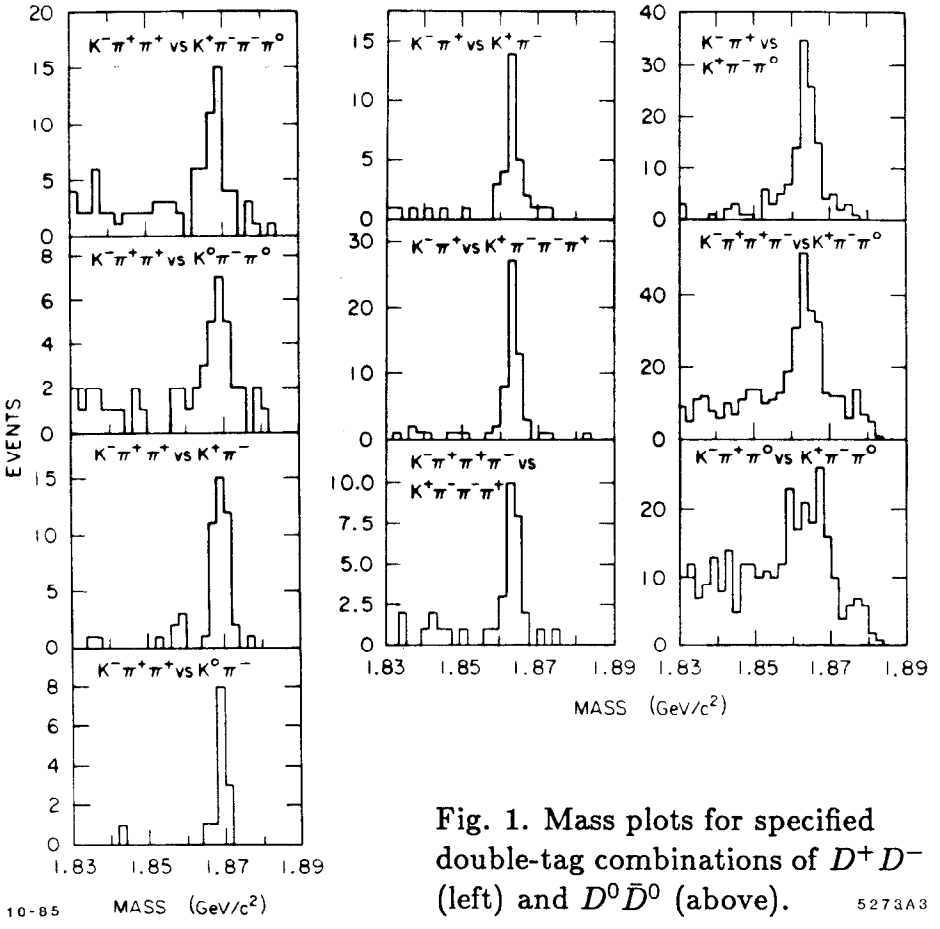

Fig. 1. Mass plots for specified double-tag combinations of D^+D^- (left) and $D^0\bar{D}^0$ (above).

The method of analysis is as follows. Let D_i be the i^{th} decay mode of a D meson. The efficiency of tagging the particular decay in the detector is ϵ_i. B_i is the branching ratio for the i^{th} final state, and $N_{D\bar{D}}$ is the number of produced $D\bar{D}$ pairs. The number of tags are given by the following equations:

$$N_{D_i} = 2\ N_{D\bar{D}}\ \epsilon_i\ B_i \qquad \text{single tags}$$
$$N_{D_jD_k} = 2\ N_{D\bar{D}}\ \epsilon_j\ B_j\ \epsilon_k\ B_k \qquad \text{double tags.}$$

The tagging efficiencies, ϵ_i, are determined by Monte Carlo simulation programs.

The numbers of events for particular decay modes, N_{D_i} and $N_{D_jD_k}$, are selected (cf Fig. 1) from the single-tag and double-tag samples. The equations are fit to the D^0 and D^+ data independently, yielding the B_i's and $N_{D\bar{D}}$.

The fits are performed on the reaction $e^-e^+ \rightarrow X\bar{X} \rightarrow$ hadronic final states, with $M_X \equiv M_{\bar{X}}$. These results do not depend on a measurement of the luminosity or on the knowledge of the shape and magnitude of the $D\bar{D}$ production cross section. The results also are nearly free from systematic errors, being dependent only on the systematic errors in the calculated tagging efficiencies. The absolute branching ratios obtained from the fits are given in the far right column of Table 1.

Table 1
Cabibbo Allowed D^0 and D^+ Branching Ratios

Decay Mode	$\sigma \cdot B$ (nb)	$B_{s.t.}$ (%)	B_{fit} (%)
$K^-\pi^+$	.237±.009±.013	4.9±0.4±0.4	5.1±0.4±0.4
$\bar{K}^0\pi^0$	.108±.020±.010	2.2±0.4±0.2	
$\bar{K}^0\eta$	.088±.039±.012	1.8±0.8±0.3	
$\bar{K}^0\omega$	.187±.073±.047	3.8±1.5±1.0	
$K^-\pi^+\pi^0$	.978±.065±.137	20.1±1.9±3.0	18.5±1.3±1.6
$\bar{K}^0\pi^+\pi^-$	.372±.030±.031	7.6±0.8±0.7	
$K^-\pi^+\pi^-\pi^+$	.566±.027±.061	11.6±1.0±1.4	11.5±0.8±0.8
$\bar{K}^0\pi^+\pi^-\pi^0$	.666±.113±.153	13.7±2.5±3.2	
$\bar{K}^0\pi^+$	.126±.012±.009	3.5±0.5±0.4	4.0±0.6±0.4
$K^-\pi^+\pi^+$	.399±.017±.028	11.1±1.4±1.2	11.3±1.3±0.8
$\bar{K}^0\pi^+\pi^0$	.714±.142±.100	19.8±4.6±3.2	14.1±2.8±2.1
$\bar{K}^0\pi^+\pi^+\pi^-$	.305±.031±.030	8.5±1.3±1.1	
$K^-\pi^+\pi^+\pi^0$	.260±.040±.054	7.2±1.4±1.6	7.5±1.5±1.6

The average luminosity for the entire run at 3.768 GeV (9325 ± 466 nb^{-1}) is determined from wide angle Bhabhas and muon pairs in our detector. From this value and the number of produced $D\bar{D}$ pairs ($22700 \pm 1600 \pm 1660$ $D^0\bar{D}^0$ and $16800 \pm 2000 \pm 1600$ $D^+\bar{D}^+$), we obtain cross sections for D^0 and D^+ production at the $\psi(3770)$: $\sigma_{D^0} = 4.9 \pm 0.3 \pm 0.4$ nb and $\sigma_{D^+} = 3.6 \pm 0.4 \pm 0.4$ nb. In Table 1 we include values of cross section times branching ratio, $\sigma \cdot B$, for a larger number of decays from a different single-tag analysis. Branching ratios for these single-tag decays, $B_{s.t.}$, are obtained by using the number of produced $D\bar{D}$ pairs given by the fits. The agreement between the branching ratios determined by the two methods is excellent.

A comparison between this experiment and other experiments performed earlier at SPEAR shows that the $\sigma \cdot B$ values for these experiments agree within

statistical errors. Thus the differences in the production cross sections between these experiments (see Table 2) are probably the causes of many of the discrepancies between our branching ratios and those of earlier experiments.

Table 2

Comparison of Energies and Cross Sections at the $\psi(3770)$

	LGW	MARK II	C.B.	MARK III
$E_{c.m.}$ (GeV)	3.774	3.771	3.771	3.768
σ_{D^0} (nb)	11.5±2.5	8.0±1.0±1.2	6.8±1.2	4.9±0.3±0.4
σ_{D^+} (nb)	9.0±2.0	6.0±0.7±1.0	6.0±1.1	3.6±0.4±0.4

3. THREE BODY HADRONIC DECAYS

We now turn to an analysis performed to isolate any pseudoscalar-vector (PV) substructure in the three body decays $D^0 \to \bar{K}^0\pi^+\pi^-$, $D^0 \to K^-\pi^+\pi^0$, and $D^+ \to \bar{K}^0\pi^+\pi^0$. Each mode is fit to a sum of interfering Breit-Wigner amplitudes (for $K^*(892)$ and ρ) and a constant amplitude for three body phase space. Appropriate phase space factors and decay angular distributions are included for the PV channels. Fits are performed using a maximum likelihood technique. As an illustration of the analysis, the Dalitz plot and $\pi^+\pi^0$ two body projection for the decay $D^0 \to K^-\pi^+\pi^0$ are shown in Fig. 2. Our results on the PV decays are summarized in Table 3. The branching ratios for the PV intermediate states

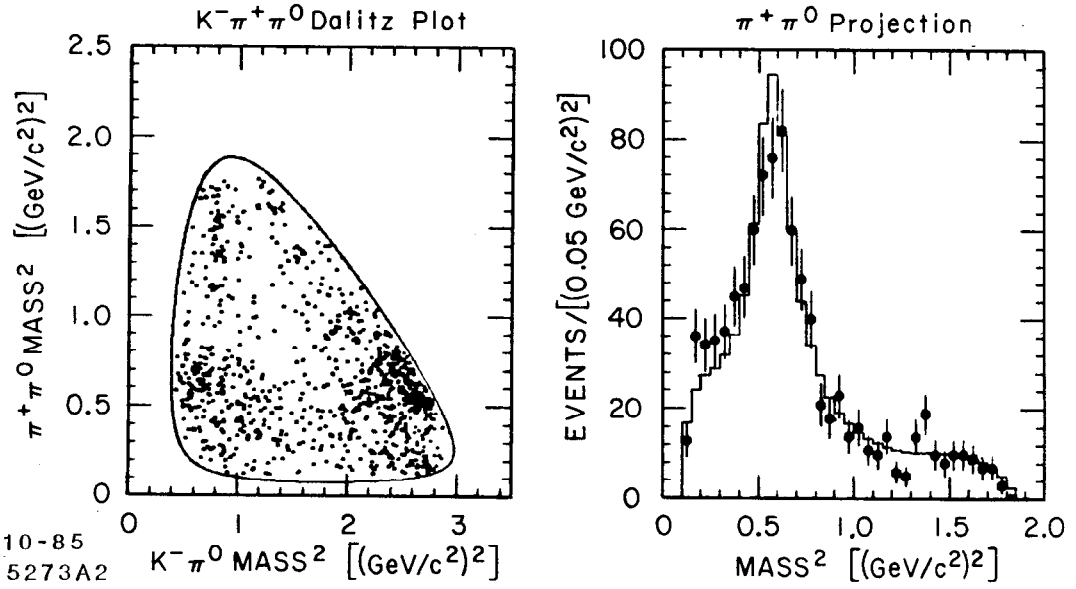

Fig. 2. (a) $D^0 \to K^-\pi^+\pi^0$ Dalitz plot. (b) $\pi^+\pi^0$ projection. The solid curve is the fit.

for $K^-\pi^+\pi^0$ and $\bar{K}^0\pi^+\pi^0$ are normalized to the double-tag fits, while the ratios for $\bar{K}^0\pi^+\pi^-$ come from the single-tag analysis using the number of produced $D^0\bar{D}^0$ pairs given by the fit. The agreement within errors of the two independent determinations of $B(K^{*-}\pi^+)$ in the $K^-\pi^+\pi^0$ and $\bar{K}^0\pi^+\pi^-$ final states provides a good check of the systematic errors in the analysis.

Table 3
Pseudoscalar-Vector Decays of D^0 and D^+

Decay Mode	Fraction (%)	$\sigma \cdot B$ (nanobarns)	B (%)
$D^0 \to K^-\pi^+\pi^0$			
$K^-\rho^+$	74.0± 6.9	.72±.07±.11	13.7±1.3±1.5
$K^{*-}\pi^+$	12.9± 3.4	.38±.09±.08	7.1±1.6±1.3
$\bar{K}^{*0}\pi^0$	7.6± 3.9	.12±.05±.03	2.1±0.9±0.6
non-resonant	5.5± 5.3	.05±.04±.03	1.0±0.8±0.6
$D^0 \to \bar{K}^0\pi^+\pi^-$			
$K^{*-}\pi^+$	63.9± 8.8	.36±.05±.04	7.3±1.2±0.9
$\bar{K}^0\rho^0$	16.8± 5.9	.06±.02±.01	1.3±0.4±0.3
non-resonant	19.3± 9.3	.07±.03±.02	1.5±0.7±0.3
$D^+ \to \bar{K}^0\pi^+\pi^0$			
$\bar{K}^0\rho^+$	86.5±10.4	.62±.14±.09	12.2±2.8±1.9
$\bar{K}^{*0}\pi^+$	7.0± 5.9	.15±.09±.09	3.0±1.9±1.7
non-resonant	6.5± 6.8	.04±.04±.03	0.9±0.8±0.6

From Tables 1 and 3, we extract the following ratios, with common systematic errors removed:

$$B(D^0 \to \bar{K}^0\pi^0)/B(D^0 \to K^-\pi^+) = 0.45 \pm 0.08 \pm 0.05$$
$$B(D^0 \to \bar{K}^{*0}\pi^0)/B(D^0 \to K^{*-}\pi^+) = 0.30 \pm 0.14 \pm 0.08$$
$$B(D^0 \to \bar{K}^0\rho^0)/B(D^0 \to K^-\rho^+) = 0.09 \pm 0.03 \pm 0.02$$

4. CABIBBO-SUPPRESSED HADRONIC DECAYS

In Table 4, we list the branching ratios for a number of Cabibbo suppressed decay modes. Some of these branching ratios have been published[2] as ratios relative to Cabibbo allowed decays. They have been converted to the values given in Table 4 through the use of the $B_{s.t.}$ values given in Table 1.

Table 4
Cabibbo Suppressed D^0 and D^+ Branching Ratios

Decay Mode	B (%)
D^0	
K^-K^+	$0.60\pm0.10\pm0.08$
$\pi^-\pi^+$	$0.16\pm0.05\pm0.03$
$\bar{K}^0K^0$	≤ 0.62
$(K^0K^-\pi^+)_{nonres}$	≤ 1.80
$\bar{K}^0K^{*0}$	≤ 0.83
$K^{*-}K^+$	$1.02\pm0.47\pm0.21$
$\pi^-\pi^+\pi^0$	$1.11^{+0.43+0.18}_{-0.35-0.18}$
$\pi^-\pi^+\pi^-\pi^+$	$1.47^{+0.61+0.19}_{-0.49-0.19}$
D^+	
$\pi^+\pi^0$	≤ 0.53
$K^+\bar{K}^0$	$1.11\pm0.34\pm0.21$
$\pi^+\pi^+\pi^-$	$0.47\pm0.19\pm0.12$
$\phi\pi^+$	$0.93\pm0.26\pm0.17$
$\bar{K}^{*0}K^+$	$0.53\pm0.24\pm0.14$
$(K^-K^+\pi^+)_{nonres}$	$0.66\pm0.30\pm0.12$

5. SEMILEPTONIC BRANCHING RATIOS

For completeness, we mention our recently published results from our measurement of the inclusive electron spectra from D^0 and D^+ decays.[3]

$$B(D^+ \to e^+ + X) = 17.0 \pm 1.9 \pm 0.7\ \%$$

$$B(D^0 \to e^+ + X) = 7.5 \pm 1.1 \pm 0.4\ \%$$

$$B(D^+ \to e^+ + X)/B(D^0 \to e^+ + X) = 2.3^{+0.5}_{-0.4} \pm 0.1$$

If we neglect the Cabibbo-suppressed semileptonic branching ratios, then the ratio of the D^+ to D^0 lifetimes equals the ratio of their respective semileptonic branching ratios.[4]

Using the single-tag sample (which contains a tag with a definite charm signature), we have reconstructed the recoil D's into the following exclusive final states:

$$D^0 \to K^-e^+\nu,\ K^-\pi^0e^+\nu,\ \bar{K}^0\pi^-e^+\nu \qquad D^+ \to \bar{K}^0e^+\nu,\ K^-\pi^+e^+\nu$$

We require (1) correct multiplicity and total charge, (2) particle identification by

time-of-flight (TOF), (3) lepton identication by TOF, shower, and muon systems, and (4) no additional gamma with energy greater than 0.100 GeV. The exclusive reconstruction process gives a very clean sample. In Table 5 we show the number of reconstructed events and branching ratios for several exclusive D meson decay modes. An examination of the $K\pi e\nu$ events shows that all are consistent with a decay through a $K^*e\nu$ intermediate state. Calling all $K\pi$ combinations K^*, and correcting for the unobserved $\bar{K}^0\pi^0e^+\nu$ state, we sum the $Ke\nu$ and $K^*e\nu$ channels and obtain:

$$B(D^+ \to \bar{K}^0e^+\nu + \bar{K}^{*0}e^+\nu) = 15.5 \pm 2.6 \pm 0.3\ \%$$

$$B(D^0 \to K^-e^+\nu + K^{*-}e^+\nu) = 7.1 \pm 1.6 \pm 0.2\ \%$$

The agreement between the inclusive and exclusive decay rates shows that there is little room left for other decay channels, and is consistent with the expected Cabibbo suppressed contribution of order $\tan^2\theta_c \approx 0.05$.

Table 5
Exclusive Semileptonic Branching Ratios

Channel	Events	Bkd. Events	B(%)
$K^-e^+\nu$	49	2.4	3.2±0.5±0.1
$K^-\pi^0e^+\nu$	4	0.0	0.9±0.5±0.1
$\bar{K}^0\pi^-e^+\nu$	5	0.0	3.0±1.4±0.2
$K^{*-}e^+\nu$			3.9±1.5±0.2
$\bar{K}^0e^+\nu$	19	0.6	9.3±2.2±0.3
$K^-\pi^+e^+\nu$	21	0.0	4.1±0.9±0.1
$\bar{K}^{*0}e^+\nu$			6.2±1.4±0.4

6. MEASUREMENT OF THE VECTOR FORM FACTOR

The decay $D^0 \to K^-e^+\nu$ can be calculated assuming that the matrix element is dominated by a single pole, where the $(c\bar{s})$ F^* is the lowest lying vector meson with the correct quantum numbers. If the mass of the electron is set to zero, then the matrix element for the decay can be written

$$M = G_F \cos\theta_c f_+(t)(P_D + P_K)^\mu \bar{u}(\nu_e)\gamma_\mu(1-\gamma_5)v(e^+).$$

In the rest frame of the D^0, where $t \equiv (P_D - P_K)^2 = m_D^2 + m_K^2 - 2m_DE_K$ and E_K is the kaon energy, we can integrate over the lepton variables and the

direction of the kaon and obtain the kaon energy spectrum:

$$W(x_K) = |f_+(t)|^2[x_K^2 - 4\lambda^2]^{3/2}$$

where $x_K = 2E_K/m_D$, $\lambda = m_K/m_D$, and $f_+(t)$ is the form factor associated with the vector part of the current. The simplest prediction for $f_+(t)$ is $f_+(t) = f_+(0)\ m_{F^*}{}^2/(m_{F^*}{}^2 - t)$. The K^- detection efficiency is flat over the low and middle t range, but falls off at large t. This falloff is due to the decay of low momenta K^-'s ($\leq 0.2\ GeV/c$) in the detector. In Fig. 3, we show the efficiency-corrected kaon energy spectrum for the 49 observed events, and the fit, calculated using the simple pole form for $f_+(t)$. The best fit value for M_{F^*} is $2.1^{+1.7}_{-0.4}$ GeV/c^2. The agreement is good, suggesting that the single vector exchange is an adequate description of the physical process.

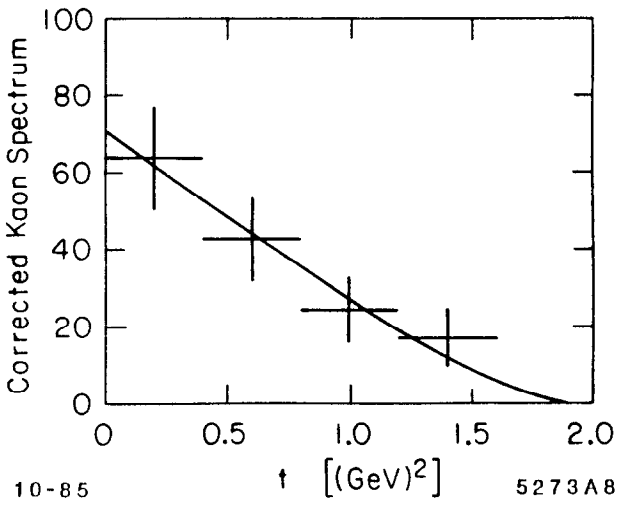

Fig. 3. Efficiency-corrected kaon energy spectrum ($W(x_K)$) and fit assuming the simple pole form for $f_+(t)$.

7. EVIDENCE FOR D$^+$ INTERFERENCE

The Cabibbo allowed spectator diagram for D^0 and D^+ decay is shown in Fig. 4(a). Fig. 4(b) shows the W exchange diagram for D^0 decay. Evidence for the existence of this diagram will be given in the next section. For certain other decay modes, two versions of the spectator diagram may exist for D^+ decays, as illustrated for a particular final state in Fig. 4(c).[5] In the presence of strong color clustering, the two distinct diagrams would result in identical final states. The distructive interference of the amplitudes for these two diagrams would reduce the D^+ hadronic width and thus lengthen its lifetime relative to the D^0. We search for this type of interference by comparing particular ratios of branching ratios.

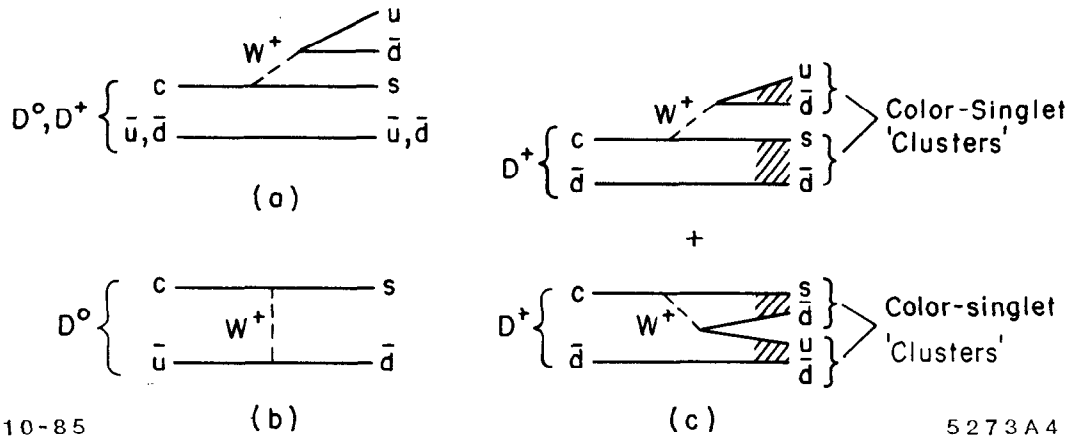

Fig. 4. Possible decay diagrams for D^0 and D^+ mesons.

The Cabibbo allowed decay $D^+ \to \bar{K}^0\pi^+$ is shown in the two diagrams of Fig. 4(c). The Cabibbo suppressed decay $D^+ \to \pi^0\pi^+$ goes by diagrams similar to those in Fig. 4(c), while the suppressed decay $D^+ \to \bar{K}^0K^+$ goes by a diagram similar to Fig. 4(a). We measure $B(D^+ \to \pi^0\pi^+)/B(D^+ \to \bar{K}^0\pi^+) \leq 0.15$ at 90% C.L. This number is based on fluctuating the one observed event to 4.2 events. The observed upper limit is consistent with the SU(3) prediction[6] of $\frac{1}{2}\tan^2\theta_c \approx 0.03$. Both decays in the ratio are reduced by the interference of diagrams like those in Fig. 4(c). On the other hand, in the ratio $B(D^+ \to \bar{K}^0K^+)/B(D^+ \to \bar{K}^0\pi^+) = 0.317 \pm 0.086 \pm 0.048$, only the decay in the denominator is reduced by the interference effect. Since the first ratio is significantly smaller than the second, this is evidence that D^+ interference is operative. We would expect the ratio $B(D^+ \to \bar{K}^{*0}K^+)/B(D^+ \to \bar{K}^{*0}\pi^+)$, for which we measure $0.18 \pm 0.14 \pm 0.11$, to behave like the ratio $B(D^+ \to \bar{K}^0K^+)/B(D^+ \to \bar{K}^0\pi^+)$. However, the accuracy of the measurement of the $B(D^+ \to \bar{K}^{*0}\pi^+)$ branching ratio is so poor that we must wait for a more accurate determination from the analysis of the three body decay $D^+ \to K^-\pi^+\pi^+$.

8. EVIDENCE FOR W EXCHANGE DIAGRAMS

The D^0 can decay, in principle, into $K^0\bar{K}^0$, $K^0\bar{K}^{*0}$, $\bar{K}^0K^{*0}$ and $\bar{K}^0\phi$ final states. The $\bar{K}^0\phi$ final state, produced through a diagram similar to that shown in Fig. 4(b), is Cabibbo allowed, but thought to be helicity suppressed at the $W\bar{u}d$ vertex. The other three decay channels are Cabibbo suppressed. In addition, $D^0 \to K^0\bar{K}^0$ is also SU(3) forbidden. Since W exchange occurs only for D^0 decays (the similar modes available to the D^+ go by W annihilation and are Cabibbo suppressed), its existence could be another of the mechanisms contributing to the non-equality of the D^0 and D^+ lifetimes.

We see one event from the decay $D^0 \to K^0\bar{K}^0$, which leads to the ratio of branching ratios:

$$B(D^0 \to K^0\bar{K}^0)/B(D^0 \to K^-\pi^+) \leq 0.11 \text{ at } 90\% \text{ C.L.}$$

We have looked in the final state ($K^0K^-\pi^+$ or $\bar{K}^0K^+\pi^-$) from D^0 decay, and have seen the distributions shown in Fig. 5. The all neutral final state, which comes only from W exchange and is therefore the more interesting, can be analyzed, leading to the following ratio of branching ratios:

$$B(D^0 \to K^{*0}\bar{K}^0 + \bar{K}^{*0}K^0)/B(D^0 \to K^-\rho^+ + K^{*-}\pi^+) \leq 0.034 \text{ at } 90\% \text{ C.L.}$$

The less interesting charged final state includes contributions from both spectator and non-spectator diagrams. Our analysis leads to the following ratio of branching ratios:

$$B(D^0 \to K^{*-}K^+ + K^{*+}K^-)/B(D^0 \to K^-\rho^+ + K^{*-}\pi^+) = 0.05 \pm 0.03.$$

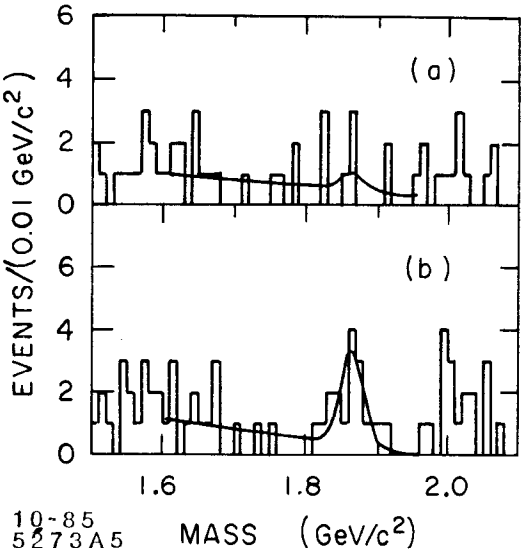

Fig. 5. (a) $\bar{K}^{*0}K^0 + \bar{K}^0K^{*0}$ (b) $K^{*-}K^+ + K^{*+}K^-$.

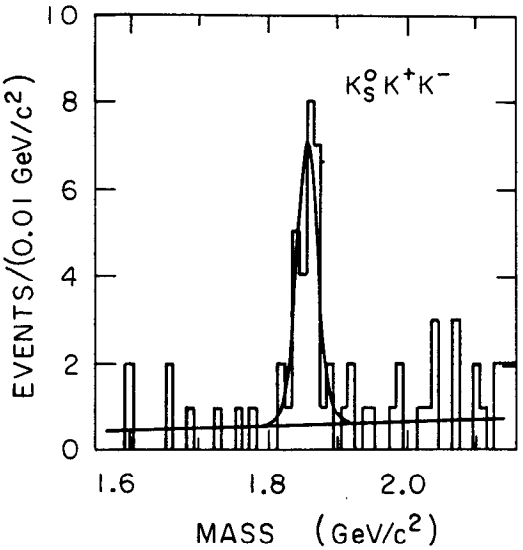

Fig. 6. $K^0_S K^+K^-$ mass distribution and fit. The background is derived from off-momentum events.

Now we turn to our search for the decay $D^0 \to \bar{K}^0\phi$. In Fig. 6 we show a mass plot for the decay $D^0 \to K^0_S K^+K^-$, where the K^0_S decays to $\pi^+\pi^-$. We observe a direct signal of 25.2 ± 5.4 events. We identify kaons by dE/dx and TOF cuts, K^0_S's by $\pi^+\pi^-$ vertex cuts, and the D^0's by the requirement that

the absolute value of the D momentum be not more than 0.050 GeV from the nominal value. The background shape is determined from off-momentum D^0's; D^0's whose momenta are between 0.060 and 0.110 GeV/c from the nominal value. A cut on the D^0 invariant mass of $\pm$ 0.040 GeV/c^2 selects 28 events, of which 4.8 $\pm$ 2.4 are background. If we then plot those 28 events as a function of the K^+K^- mass, we find 4 events below, 11 events within, and 13 events above the ϕ region (1.019 $\pm$ 0.015 GeV/c^2). These events are plotted in Fig. 7.

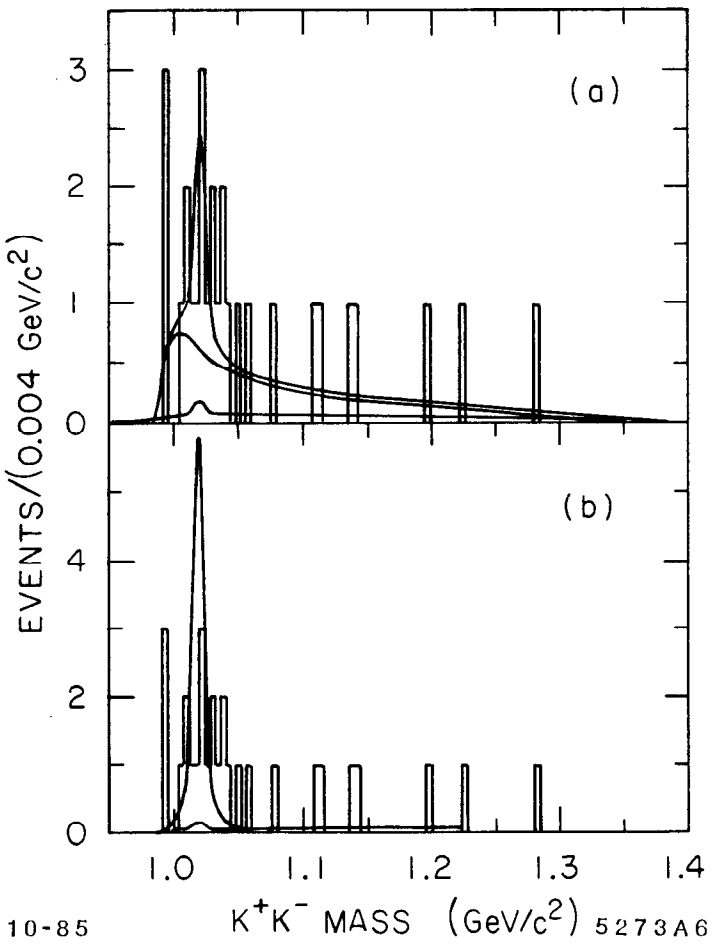

Fig. 7. (a)K^+K^- mass in $K^0_S K^+K^-$, with fit including background, $\bar{K}^0\phi$ and $\bar{K}^0\delta^0$. (b) As in (a) except for upper limit assuming only $\bar{K}^0\phi$ and background.

A number of processes have been considered that might contribute backgrounds to $\bar{K}^0K^+K^-$, and specifically into the ϕ region as defined above. Except for the decay mentioned below, we have found no processes that can feed large contributions into the ϕ region. We have no experimental information about the decay $D^0 \to \bar{K}^0\delta^0$. However, a Monte Carlo simulation of this decay, using the

Flatte parameterization[7] of the δ^0, leads to a peak at low K^+K^- mass and a long tail into the high mass region. In Fig. 8 we show the Dalitz plot for the 28 events in the $\bar{K}^0K^+K^-$ state, and 400 Monte Carlo events each in the $\bar{K}^0\delta^0$ and $\bar{K}^0\phi$ final states. The latter Monte Carlo shows the strong angular distribution expected from the pseudoscalar-vector decay. Additional Monte Carlo efficiency studies indicate no significant distortion of the K^+K^- mass distribution near threshold, for pseudoscalar or vector parents. The Monte Carlo results suggest that the high mass tail cannot be ignored but needs to be extrapolated into the low mass region. Our conclusion is that the observed distribution favors the ϕ and a low mass K^+K^- enhancement.

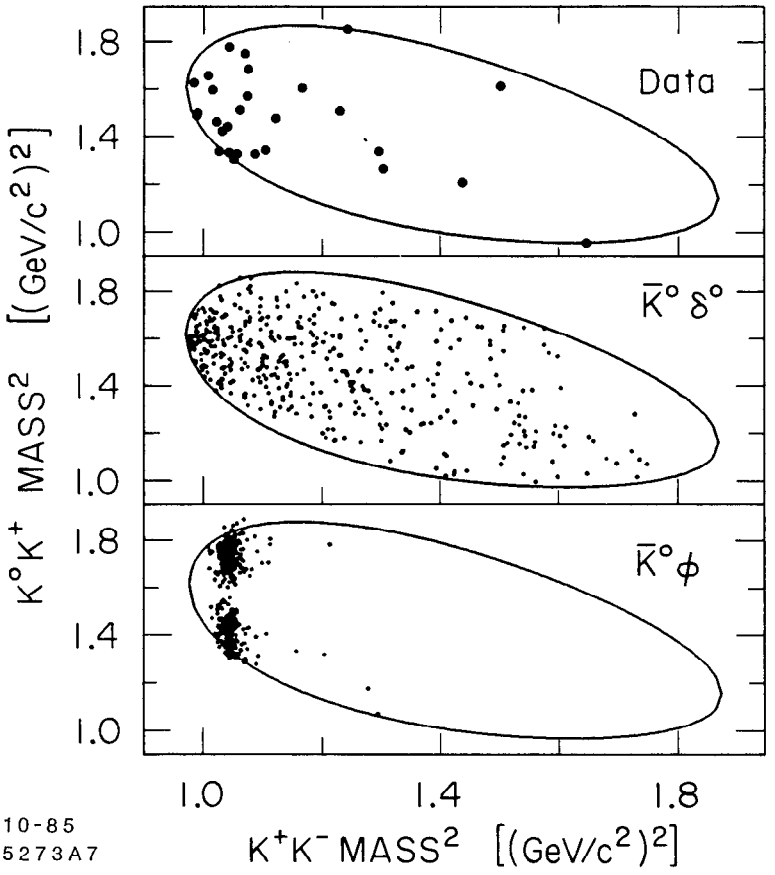

Fig. 8. Dalitz plots for $K^0_SK^+K^-$ data, and $\bar{K}^0\delta^0$ and $\bar{K}^0\phi$ Monte Carlo predictions.

In Fig. 7, we compare the data with two different fits to signal plus background. From a fit that includes contributions from $\bar{K}^0\delta^0$ and non-resonant background (Fig. 7a), we obtain 5.2 ± 3.3 events from the decay $D^0 \to \bar{K}^0\phi$. This translates to a branching ratio $B(D^0 \to \bar{K}^0\phi) = 0.7 \pm 0.5 \pm 0.2\%$. Alternatively, we obtain an upper limit ignoring both the low mass events and the high mass

tail but including a contribution from a non-resonant background (Fig. 7b):

$$B(D^0 \to \bar{K}^0\phi) \leq 2.5\% \text{ at } 90\% \text{ C.L.}$$

This result is based on 17.5 events (including contributions from systematic errors).

9. CONCLUSIONS

We summarize the new results from the MARK III collaboration:

(a) We have made high statistics measurements of the absolute D meson branching ratios. These are independent of cross section measurements.

(b) We have presented measurements of $D \to (e + X)$ and the ratio of the D^+ to D^0 lifetimes. The error in the lifetime ratio is comparable with the error in the ratio of the world averages of the direct D^+ and D^0 lifetimes.

(c) We have presented new measurements of $D \to Ke\nu$ and $D \to K^*e\nu$, and the f_+ vector form factor.

(d) We have made measurements of a large number of D branching ratios. We can account for about 85% of all D^+ and D^0 decays.

(e) We have presented evidence for D^+ interference.

(f) We have presented evidence for the existence of non-spectator diagrams. There appear to be other structures present in the $\bar{K}^0K^+K^-$ final state at high and low K^+K^- mass that are inconsistent with background, and feed into the low K^+K^- mass region.

10. ACKNOWLEDGEMENTS

I would like to thank Hai-Yang Cheng for a number of discussions concerning the interpretation of our data, and G. T. Blaylock, D. Coffman, and R. H. Schindler for help in the preparation of this paper. This work was supported in part by the U.S. National Science Foundation and the U.S. Department of Energy under Contracts No. DE-AC03-76SF00515, No. DE-AC02-76ER01195, No. DE-AC03-81ER40050, and No. DE-AM03-76SF00034.

11. REFERENCES

[1]D. Bernstein *et al.*, Nucl. Instrum. Methods **226**, 301 (1984).
[2]R. M. Baltrusaitis *et al.*, Phys. Rev. Lett. **55**, 150 (1985).
[3]R. M. Baltrusaitis *et al.*, Phys. Rev. Lett. **54**, 1976 (1985).
[4]A. Pais and S. B. Treiman, Phys. Rev. D **15**, 2529 (1977).
[5]B.Guberina *et al.*, Phys. Lett. **89B**, 111 (1979).
[6]R. L. Kingsley *et al.*, Phys. Rev. D **11**, 1919 (1975).
[7]S. M. Flatte, Phys. Lett. **63B**, 224 (1976).

SLAC – PUB – 3818
December 1985
(E)

ERRATUM

RECENT RESULTS ON D MESON DECAYS FROM THE MARK III*

David H. Coward
Stanford Linear Accelerator Center
Stanford University, Stanford, California 94305

Representing the MARK III Collaboration

A typographical error has been discovered in Table 1. The first decay mode should be listed as $K^-\pi^+$ instead of $K^+\pi^-$. Please correct your copy of the SLAC-PUB.

Table 1
Cabibbo Allowed D^0 and D^+ Branching Ratios

Decay Mode	$\sigma \cdot B$ (nb)	$B_{s.t.}$ (%)	B_{fit} (%)
$K^-\pi^+$	.237±.009±.013	4.9±0.4±0.4	5.1±0.4±0.4
$\bar{K}^0\pi^0$	.108±.020±.010	2.2±0.4±0.2	
$\bar{K}^0\eta$	.088±.039±.012	1.8±0.8±0.3	
$\bar{K}^0\omega$	.187±.073±.047	3.8±1.5±1.0	
$K^-\pi^+\pi^0$	.978±.065±.137	20.1±1.9±3.0	18.5±1.3±1.6
$\bar{K}^0\pi^+\pi^-$	.372±.030±.031	7.6±0.8±0.7	
$K^-\pi^+\pi^-\pi^+$	.566±.027±.061	11.6±1.0±1.4	11.5±0.8±0.8
$\bar{K}^0\pi^+\pi^-\pi^0$	.666±.113±.153	13.7±2.5±3.2	
$\bar{K}^0\pi^+$	.126±.012±.009	3.5±0.5±0.4	4.0±0.6±0.4
$K^-\pi^+\pi^+$	.399±.017±.028	11.1±1.4±1.2	11.3±1.3±0.8
$\bar{K}^0\pi^+\pi^0$	.714±.142±.100	19.8±4.6±3.2	14.1±2.8±2.1
$\bar{K}^0\pi^+\pi^+\pi^-$	.305±.031±.030	8.5±1.3±1.1	
$K^-\pi^+\pi^+\pi^0$	.260±.040±.054	7.2±1.4±1.6	7.5±1.5±1.6

Invited talk presented at the Annual Meeting of the Division of Particles and Fields of the APS, Eugene, Oregon, August 12-15, 1985

* Work supported in part by the National Science Foundation and by the Department of Energy, contracts DE-AC03-76SF00515, DE-AC02-76ER01195, DE-AC03-81ER40050, and DE-AM03-76SF00034.